Desalination and Water Treatment
www.deswater.com
doi: 10.1080/19443994.2013.787551

52 (2014) 238–247
January

Taylor & Francis
Taylor & Francis Group

Effective decolorization of congo red in aqueous solution by adsorption and photocatalysis using novel magnetic alginate/ γ-Fe_2O_3/CdS nanocomposite

Ru Jiang[a,b], Jun Yao[a], Huayue Zhu[a,b,*], Yongqian Fu[a], Yujiang Guan[a], Ling Xiao[b], Guangming Zeng[c,*]

[a]*Department of Environmental Engineering, Laboratory of Resource Utilization and Pollution Control, Taizhou University, No.1139, Municipal Government Avenue, Jiaojiang District, Taizhou 318000, Zhejiang, P.R. China*
Tel. +86 0139 8967 2070; Fax: +86 0576 8513 7066; email: zhuhuayue@126.com
[b]*Key Laboratory for Biomass-Resource Chemistry and Environmental Biotechnology of Hubei Province (Wuhan University), Wuhan 430072, Hubei, P.R. China*
[c]*Key Laboratory of Environmental Biology and Pollution Control (Hunan University), Ministry of Education, Changsha 410082, Hunan, P.R. China*
Tel. +86 731 8822 754; Fax: +86 731 8823 701; email: zgming@hnu.cn

Received 10 November 2012; Accepted 2 March 2013

ABSTRACT

Magnetic alginate/γ-Fe_2O_3/CdS composite photocatalyst (m-alginate/Fe_2O_3/CdS composite) was synthesized via a simple hydrothermal method, and characterized by X-ray diffraction (XRD), thermogravimetric analysis (TGA), differential thermal analysis (DTA), and vibrating sample magnetometer (VSM). The photocatalytic activity of m-alginate/Fe_2O_3/CdS composite was evaluated via the adsorption-photocatalytic removal of aqueous organic dye, i.e. congo red (CR). The m-alginate/Fe_2O_3/CdS composite can be easily manipulated and separated by a magnetic field, leading to the convenience and feasibility in the removal of aqueous hazardous dye. In addition, the kinetics of photocatalysis of CR has also been performed and found to follow the pseudo-first-order kinetics. These results suggest that m-alginate/Fe_2O_3/CdS composite can be used as an effective photocatalyst for the removal of hazardous pollutants such as dyes, and the adsorption-photocatalysis of these organic contaminants in wastewater effluents can solve one of the most important environmental problems in the related industry. This opens new perspectives for the preparation of magnetic photocatalyst based on biopolymers and effective treatment of aqueous hazardous dye.

Keywords: Decolorization; Water treatment; CR; Adsorption; Photocatalysis; Alginate/ γ-Fe_2O_3/CdS

1. Introduction

Textile and tannery effluents are two of the most important industrial effluents, and the problems of treatment and disposal of such effluents require much attention [1]. A range of physicochemical methods have been suggested and applied for the removal of hazardous organics dyes from those effluents, such as adsorption [2,3], heterogeneous photocatalysis [4–6],

*Corresponding author.

and coagulation/flocculation [7]. Heterogeneous photocatalysis using suited semiconductor is a general and efficient method for the removal of aqueous organic dyes pollutants. The expansion and the technological application of heterogeneous photocatalysis require the development of efficient and suited photocatalysts [8]. Among the reported photocatalysts with visible light response, CdS has a relatively narrow band gap energy of 2.42 eV (300 K), corresponding well to the spectrum of sunlight and, therefore, is regarded as one of the most attractive visible light-driven photocatalysts [9–11]. However, CdS is prone to conglomeration during preparation via a conventional method and photocorrosion during the photochemical reaction, since CdS itself is oxidized by the photogenerated holes [9]. In addition, powdery nanosized CdS photocatalyst is also difficult to be separated from the treated solution, except high speed centrifugation, thus its application in wastewater treatment is further limited.

Polymer/inorganic composite materials have attracted much attention recently because they exhibit superior characters, such as magnetic, electrical, and optical properties, combining organic and inorganic materials properties [2,4,12]. The strong affinity of some biopolymers with metal ions makes them quite suitable as host matrices for the embedment of certain semiconductor photocatalysts (e.g. TiO_2, CdS, and TiO_2/CdS composite) [5,12,13]. Some recent researches reported by Albert and Wendy, indicated that organic biopolymer such as matrices of semiconductor also provide an interface for the charge transfer, and thus for the improvement of photocatalytic efficiency [14,15]. Among those biopolymers, one of the most widely studied biopolymers is polysaccharide such as alginate, which is a natural polysaccharide extracted from various species of brown seaweed. It consists of linear copolymers composed of β-D-Mannuronate (M) and α-L-Guluronate (G), linked by α-1,4- and a-1,4-glycosidic bonds [16]. The inorganic semiconductors/alginate composite materials can be considered as a portable photocatalyst for the removal of aqueous organic dye, since alginate has excellent binding sites for divalent cations because of the presence of amino, carboxyl, phosphate, and sulfate functional groups within it [17–20]. In addition, magnetic separation is considered as a high speed and effective technique for separating powdery polymer–inorganic composite materials [2]. Therefore, if powdery photocatalyst is magnetic, it could be recovered conveniently by magnetic separation technology [2,11,21]. Due to its excellent magnetic properties, chemical stability, and biocompatibility, γ-Fe_2O_3 has been widely used in magnetic adsorbents [2], isolation of plasma DNA [22], sensors [23], and other fields. Recent research also indicated that the enhanced photocatalytic activity under visible light ($\lambda > 420$ nm) was observed in 1D CdS/Fe_2O_3 heterostructures due to fast charge separation [11]. Therefore, it is of fundamental importance to develop convenient, economic, and efficient methods for the preparation of novel magnetic composite photocatalyst based on alginate. However, to our knowledge, there has been no report regarding the preparation of CdS/γ-Fe_2O_3 immobilized on alginate matrix, especially their photocatalytic ability in the removal of aqueous organic dye by adsorption-photocatalytic process under visible light irradiation.

In this study, the objective is to evaluate the practicability and potential use of a magnetic alginate/γ-Fe_2O_3/CdS composite photocatalyst (m-alginate/Fe_2O_3/CdS composite) as an effective adsorbent for the treatment of containing-dye waste water. Congo red (CR) was chosen as a model aqueous organic dye. The effects of photocatalyst dosage and initial CR concentration on photocatalytic decolorization of the dye solution were also studied. The results obtained from the present study could provide fundamental information for the design of such a process for the photocatalytic treatment of azo-dye-contaminated industrial effluents.

2. Experimental

2.1. Chemicals

Sodium alginate was of reagent grade (300–400 CP) purchased from Shanghai Chemical Reagent Co., Ltd. (Shanghai, China) and used without further purification. Commercially available maghemite γ-Fe_2O_3 (20–30 nm outer diameters; 98% purity) was obtained from Tongrenweiye Technology Co., Ltd. (Shijiazhuang, China). CR ($C_{32}H_{22}N_6O_6S_2Na_2$, mol. wt. 696.67) was purchased from Yongjia Fine Chemical Factory (Whenzhou, China) and used as received without further purification. Fig. 1 displays the molecular structure of the dye. $Cd(NO_3)_2$ and sulfocarbamide ($(NH_2)_2CS$) were used as precursors of crystalline CdS. All other reagents used are of analytical reagent grade.

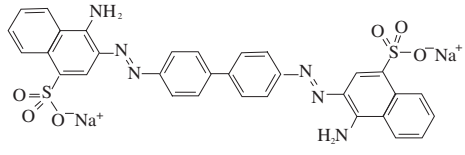

Fig. 1. Molecular structure of CR.

2.2. Preparation of m-alginate/Fe_2O_3/CdS composite

Fig. 2 illustrates the preparation procedure of m-alginate/Fe_2O_3/CdS composite. Alginate gel solution was prepared by dissolving and gently heating 1 g of sodium alginate in 50 mL of double- distilled water. About 2.284 g of $CdCl_2$ was dissolved in 100 mL of double- distilled water to obtain 0.1 M of Cd^{2+} aqueous solution. Then, sodium alginate gel solution, Cd^{2+} aqueous solution, and 0.5 g of γ-Fe_2O_3 were mixed under continuous mechanical stirring at room temperature. After stirring for 12 h, obtained viscous dispersoid was introduced dropwise using a syringe into a $CaCl_2$ bath (200 mL, 2% m/v) and spherical alginate/Fe_2O_3 hydrogel beads containing Cd^{2+} ions (alginate/Fe_2O_3/Cd^{2+} beads) were formed instantaneously. The suspension of hydrogel beads was then allowed to stand and age for 2 h in the $CaCl_2$ bath without agitation at room temperature. After separated and rinsed with deionized water three times, the microbeads were immersed into 0.03 mol L^{-1} of $(NH_2)_2CS$ solution, while 0.5 mol L^{-1} of NaOH solution (40 mL) was added dropwise to the reaction to adjust pH to 11 and stirred for 1 h at 70 ± 0.5°C. The hydrolysis reactions of sulfocarbamide in an alkali medium took place at 70°C as described in Eqs. (1) and (2) [24]. Cd^{2+} ions in alginate/Fe_2O_3/Cd^{2+} beads reacted with S^{2-} released slowly from fresh sulfocarbamide to form crystalline CdS, according to Eq. (3) [5]. The alginate/Fe_2O_3/CdS hydrogel beads was aged at 70°C for 4 h and washed with double distilled water three times. The alginate/Fe_2O_3/CdS hydrogel beads were then placed in a Petri dish and dried in an oven at 60°C for 2 days. Finally, alginate/Fe_2O_3/CdS hydrogel beads were triturated to obtain powdery alginate/Fe_2O_3/CdS composite photocatalyst.

$$(NH_2)_2CS + OH^- \rightarrow CH_2N_2 + H_2O + HS^- \quad (1)$$

$$HS^- + OH^- \rightarrow S^{2-} + H_2O \quad (2)$$

$$\text{m-alginate beads–}Cd^{2+} + S^{2-} \rightarrow \text{m-Alginate beads–CdS} \downarrow \quad (3)$$

2.3. Characterization of m-alginate/Fe_2O_3/CdS composite

X-ray diffraction (XRD) patterns were obtained by a model D8-Advance Bruker X-ray diffractometer using Cu Kα radiation ($\lambda = 0.15406$ nm) at 40 kV and 40 mA. The scanning rate was 2 min^{-1} and the scanning scope of 2θ was from 10 to 70 in a fixed time mode with a step interval of 0.02 at room temperature.

Dynamic thermogravimetric analysis (TGA) was carried out by SDT Q 600 thermogravimetric analyzer (USA). About 12–20 mg of dry materials was ground into powder, and then placed in a platinum pan and heated from 20 to 750°C at a rate of 10°C min^{-1} under a dynamic nitrogen atmosphere flowing at 100 mL min^{-1}. Magnetization measurements were performed at 298 K in magnetic fields ± 10 kOe using a model HH-15 vibrating sample magnetometer (Nanjing, China). High-resolution transmission electron microscopy (HRTEM) images were observed on a JEOL JEM-2010 electron microscope using an accelerating voltage of 200 kV (Japan). Photos of solution before and after magnetic separation were taken using a Cannon IXUS 95 IS digital camera (Japan).

2.4. Adsorption experiments

Adsorption experiments were performed on a model KYC-1102 C thermostate shaker (Ningbo, China) with a shaking speed of 100 rpm. The CR solution was prepared by dissolving CR powder in double distilled water to obtain a solution with a concentration of 20 mg L^{-1}. A 100 mL of CR solution and 0.05 g of m-alginate/Fe_2O_3/CdS composite were added into 250 mL glass flask and then shook at 25 ± 0.5°C. At desired time intervals, about 5 mL of the solution was taken and m-alginate/Fe_2O_3/CdS

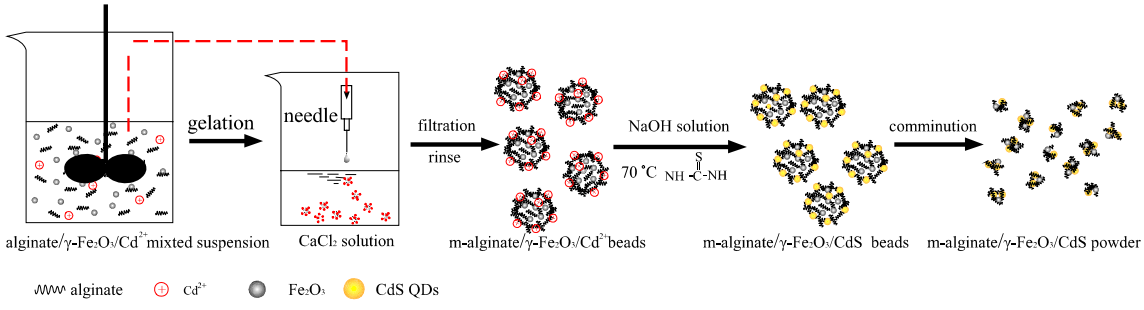

Fig. 2. Schematic illustration of the preparation of m-alginate/Fe_2O_3/CdS composite.

Table 1
Typical experimental conditions for photocatalytic decolorization of CR aqueous solution

Parameter	Condition
Initial concentration of CR	20 mg L^{-1}
Reaction temperature	25 ± 1℃
Flow rate of air	100 mL min^{-1}
Photocatalyst dosage	0.5 g L^{-1}

composite was removed from the solution by magnetic separation.

2.5. Photocatalytic experiments

The typical experimental conditions on photocatalytic experiments are summarized in Table 1.The visible light irradiation was provided by a model PLS-SXE300 300 W xenon lamp (Beijing Trusttech Co., Ltd. China) and an appropriate cutoff filter was placed in the front of the reactor to remove the part of UV radiation. About 0.05 g of photocatalyst was suspended in 100 mL of CR dye solution with an initial concentration of 20 mg L^{-1}. During the photocatalytic decolorization of CR dye, the reaction solution was continuously aerated by a pint-sized pump for providing enough oxygen and complete mixing of reaction solution.

In order to compare, direct photolysis experiment of CR dye solution has been carried out under the same light irradiation.

2.6. Magnetic separation of photocatalyst

At every predetermined time interval, 5 ml of samples was then withdrawn regularly from the reactor and all suspended photocatalysts were immediately removed from the treated solution by placing an external magnetic field.

2.7. Analysis of CR solution

The clean transparent solution was analyzed by a Cary 50 UV–vis spectrophotometer. The full spectrum (200–750 nm) for each sample was recorded and the absorbance at maximal characteristic band at 496 nm was followed to determine the CR concentration. A calibration plot based on Beer–Lambert's law was established by relating the absorbance to the concentration.

3. Results and discussion

3.1. Characterization of m-alginate/Fe_2O_3/CdS composite

XRD was performed to examine the crystal structures of alginate, γ-Fe_2O_3 and m-alginate/Fe_2O_3/CdS composite. The results are shown in Fig. 3. The diffraction pattern of alginate showed a typical peak around 13.72° [25,26]. Diffraction peaks of magnetic γ-Fe_2O_3 nanoparticles at 2θ of 30.06°, 35.44°, 53.66°, 57.14°, and 62.76° corresponded to (220), (311), (422), (511), and (440) lattice planes of γ-Fe_2O_3 (Fig. 3(b)), which was consistent with the database of maghemite (γ-Fe_2O_3) (JCPDS No. 39-1346) [27,28]. According to the Scherrer's equation, calculated average crystallite size of magnetic γ-Fe_2O_3 nanoparticles was about 20 nm, which agreed basically with the mean diameter (25 nm) of the TEM (shown in the inset (b) of Fig. 5). All characteristic diffraction peaks of magnetic γ-Fe_2O_3 could also be found in XRD patterns of m-alginate/Fe_2O_3/CdS composite (Fig. 3(c)), indicating that the fabrication of m-alginate/Fe_2O_3/CdS composite did not change the chemical structure of magnetite (γ-Fe_2O_3). In addition, the peaks located at 26.48°, 43.22°, and 52.22° could be indexed to the reflection from (002), (1 1 0), (1 1 2), and (1 0 4) planes of hexagonal phase CdS (JCPDS No. 01-080-0006), respectively. However, the typical peaks of alginate around 13.72° disappeared entirely with the addition of γ-Fe_2O_3 and crystalline CdS, which could be explained from the fact that intermolecular interaction destroyed the regularity of alginate by binding with Cd^{2+} during the preparation of m-alginate/Fe_2O_3/CdS composite.

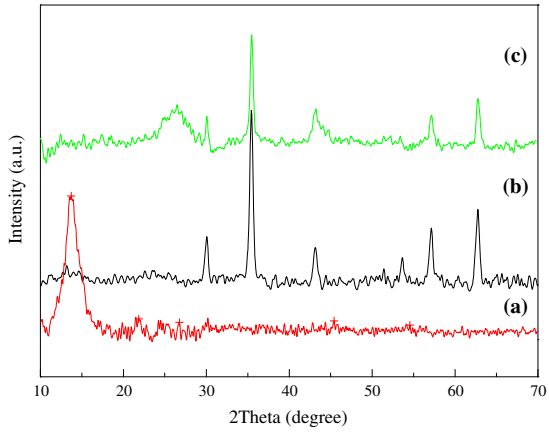

Fig. 3. XRD patterns of alginate (a), γ-Fe_2O_3 (b), and m-alginate/Fe_2O_3/CdS composite (c).

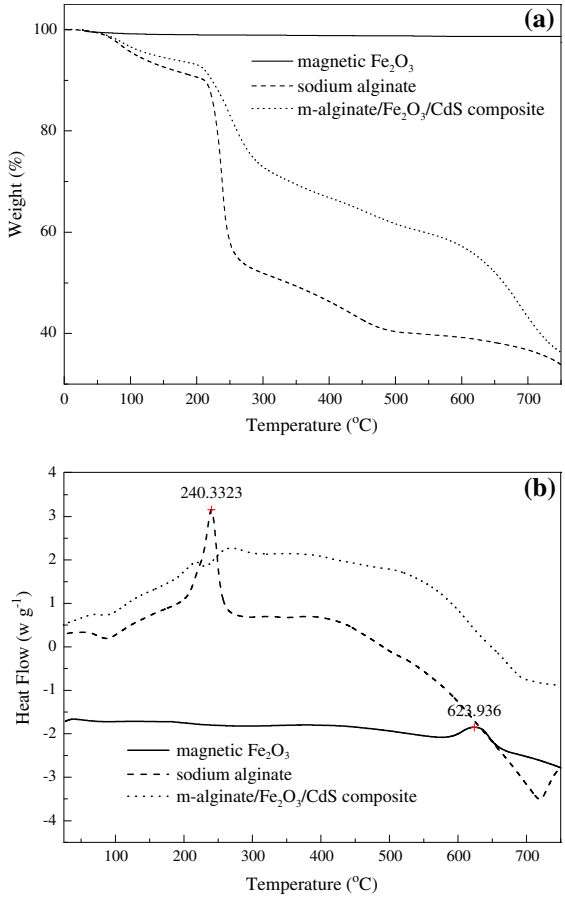

Fig. 4. TGA (a) and DSC, (b) patterns of magnetic γ-Fe_2O_3, sodium alginate, and m-alginate/Fe_2O_3/CdS composite.

The thermal analysis of samples was performed in the range 25–750°C using DTA-TG analysis and the results are illustrated in Fig. 4. Pure alginate showed an endothermic peak at 88.59°C that was due to loss of moisture, and a distinct exothermic peak located at 240°C that was attributed to the decomposition of the molecular side chains [29]. The weight loss of 66 wt.% at 750°C was mainly due to the decomposition of alginate [22]. For raw nanosized γ-Fe_2O_3, no significant weight loss was observed in the TGA curve (Fig. 4(a)) from 25°C to 750°C. However, there was an obvious exothermic peak at 624°C in the DTA curve, which represented the phase transition from γ-Fe_2O_3 to α-Fe_2O_3 [23]. The differential thermal analysis (DTA) of m-alginate/Fe_2O_3/CdS composite showed no obvious endothermic peaks in the range 25–750°C. Especially, the obvious exothermic peak at 624°C of that represented the phase transition from γ-Fe_2O_3 to α-Fe_2O_3 disappeared in the DTA curve of m-alginate/Fe_2O_3/CdS composite, implying that thermal stability of γ-Fe_2O_3 in m-alginate/Fe_2O_3/CdS composite

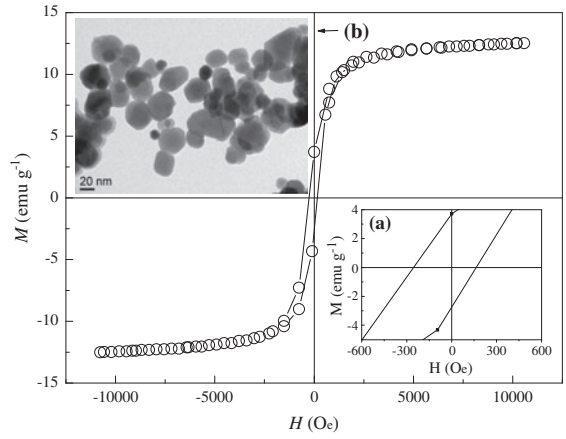

Fig. 5. Magnetization curve of m-alginate/Fe_2O_3/CdS composite. Insets: (a) low field magnetization curve at 298 K, and (b) HRTEM photo of γ-Fe_2O_3.

enhanced by combination with amino, carboxyl, phosphate, and sulfate functional groups in alginate chains.

A magnetic hysteresis loop of m-alginate/Fe_2O_3/CdS composite at a magnetic field of ± 10,000 Oe at 298 K is shown in Fig. 5. Obviously, its magnetization under the applied magnetic field at 298 K exhibited a hysteresis loop with the remanent magnetization (M_r) and coercivity (H_c) of 3.71 emu g^{-1} and 163.64 Oe (see the inset (a) of Fig. 5), respectively, indicating that the m-alginate/Fe_2O_3/CdS composite did not show super paramagnetic property at room temperature. It is well known that superparamagnetic behavior was observed for magnetic nanoparticles with sizes less than 10 nm. However, the diameter of γ-Fe_2O_3 nanoparticles in m-alginate/Fe_2O_3/CdS composite was in the range 18–30 nm (shown in the inset (b) of Fig. 5). At the same time, m-alginate/Fe_2O_3/CdS composite exhibited a saturation magnetization value (M_s) of 12.43 emu g^{-1}, at an applied magnetic field of ± 10,000 Oe, in comparison with the theoretical saturation magnetization of 76 emu g^{-1} for bulk γ- Fe_2O_3 at room temperature [30].

Furthermore, the magnetic separability of m-alginate/Fe_2O_3/CdS composite was tested by placing an external magnetic field. The m-alginate/Fe_2O_3/CdS composite was attracted toward the magnet within 30 s whether the magnet was beside or under the cuvette (Fig. 6(b and c)), indicating that the m-alginate/Fe_2O_3/CdS composite still had strong magnetic response to an external magnetic field. This presented an easy and efficient way to separate m-alginate/Fe_2O_3/CdS composite from a treated solution system under an external magnetic field.

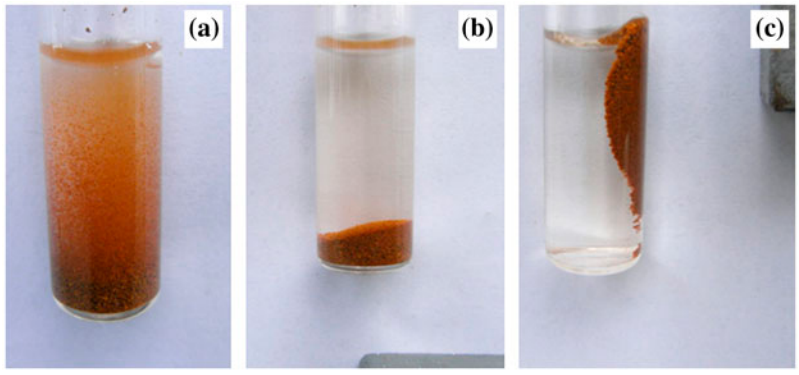

Fig. 6. The suspension (a) of m-alginate/Fe_2O_3/CdS composite and its response (b and c) to the applied magnetic field at 298 K.

3.2. Adsorption kinetics of CR onto m-alginate/Fe_2O_3/CdS composite

It is well known that adsorption of reactants on photocatalyst surface is the first step in a photocatalytic reaction [31]. Since the photocatalytic degradation of dyes occurs predominantly on the photocatalyst surface, study of the adsorption of CR from aqueous solution onto m-alginate/Fe_2O_3/CdS composite is important. Therefore, the kinetic parameters are helpful for the prediction of treatment rate, which gives important information for designing and modelling adsorption-photocatalytic processes. In order to investigate the controlling mechanism of adsorption processes, such as transfer and chemical reaction, two different linear kinetic models, i.e. the Lagergren-first-order model (Eq. (4)) [32] and pseudo-second-order model (Eq. (5)) [33], were applied to model the kinetics of CR adsorption onto m-alginate/Fe_2O_3/CdS composite.

$$\log(q_e - q_t) = \log q_e - \frac{k_1 t}{2.303} \tag{4}$$

$$\frac{t}{q_t} = \frac{1}{k_2 q_e^2} + \frac{1}{q_e} t \tag{5}$$

where q_e and q_t are amounts of CR (mg g^{-1}) adsorbed on adsorbent at equilibrium and at a given time t, respectively; k_1 is the rate constant (min^{-1}) of Lagergren-first-order kinetic model for adsorption, k_2 is the rate constant (g mg^{-1} min^{-1}) of pseudo-second-order kinetic model for adsorption. Values of k_1 can be calculated from the plots of $\log(q_e - q_t)$ vs. t for Eq. (4). The slope and intercept of the linear plots of t/q_t against t yield the values of $1/q_e$ and $1/k_2 q_e^2$ for Eq. (5).

Plots of $\log(q_e - q_t)$ vs. t and $t/(q_t)$ vs. t are shown in Fig. 7, and corresponding kinetic parameters are listed in Table 2. The value of correlation coefficient (R^2) value for Eq. (4) is near 1 which is larger than that of Eq. (5). Moreover, the $q_{e,\ exp}$ value was much closer to the $q_{e,\ cal}$ value calculated by Eq. (4) than by Eq. (5) (Table 2). These results showed that the adsorption of CR on m-alginate/Fe_2O_3/CdS composite obeyed the Lagergren-first-order kinetic model. A similar phenomenon has been observed in the adsorption of acid dyes by CS/CNT beads [3].

3.3. Removal of CR by adsorption-photocatalytic process

To demonstrate the potential applicability of the prepared m-alginate/Fe_2O_3/CdS composite as photocatalyst under visible light irradiation, its photocatalytic

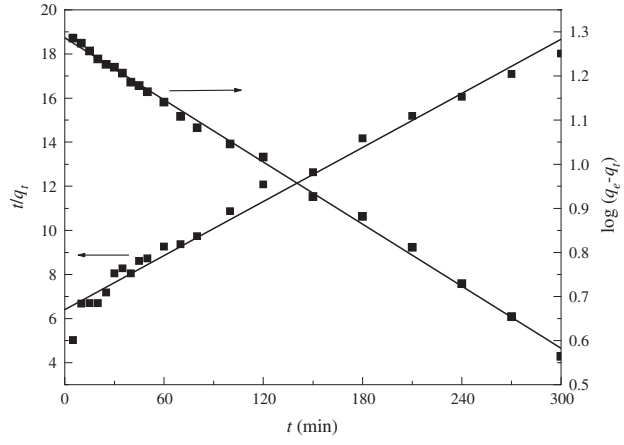

Fig. 7. Lagergren-first-order kinetic and pseudo-second-order kinetic plots for CR adsorption onto m-alginate/Fe_2O_3/CdS composite at 298 K (Catalyst dosage: 0.5 g L^{-1}; CR concentration: 20 mg L^{-1}).

Table 2
Kinetic parameters of CR adsorption onto m-alginate/Fe_2O_3/CdS composite at 298 K

C_0 (mg L^{-1})	$q_{e,exp}$ (mg g^{-1})	Lagergren-first-order kinetic model			Pseudo-second-order kinetic model		
		$q_{e,cal}$ (mg g^{-1})	k_1 (min^{-1})	R^2	$q_{e,cal}$ (mg g^{-1})	k_2 (g mg^{-1} min^{-1})	R^2
20	20.31	20.46	0.00235	0.998	16.07	0.04088	0.982

activity was studied through the degradation of CR in aqueous solution. About 91.57% decolorization of CR solution took place after 300 min of direct photolysis experiment in the presence of m-alginate/Fe_2O_3/CdS composite, while 1.37% decolorization under direct photolysis experiment (figure now shown). As a result, m-alginate/Fe_2O_3/CdS could effectively promote photocatalytic decolorization of CR. Fig. 8 displays the temporal evolution of the spectral changes during the photodegradation of CR aqueous solution (20 mg L^{-1}) over the m-alginate/Fe_2O_3/CdS composite (0.5 g L^{-1}) at different irradiation time. CR showed three major absorption bands, which was characterized by one main band in the visible region with its maximum absorption at 496 nm and by other two bands in the ultraviolet region located at 236 and 341 nm, respectively (Fig. 8). The absorbance peaks at 236 and 341 nm were attributed to "benzene and naphthalene rings" structures, while the absorbance peak at 496 nm was attributed to the azo bonds of CR molecule [34]. The rapid decrease in the intensity of 496 nm band in Fig. 8 indicated that the chromophore responsible for characteristic color of the CR solution was broken down. It has been reported that the break-up of the N = N bond, responsible for the coloration of the azo compounds, is

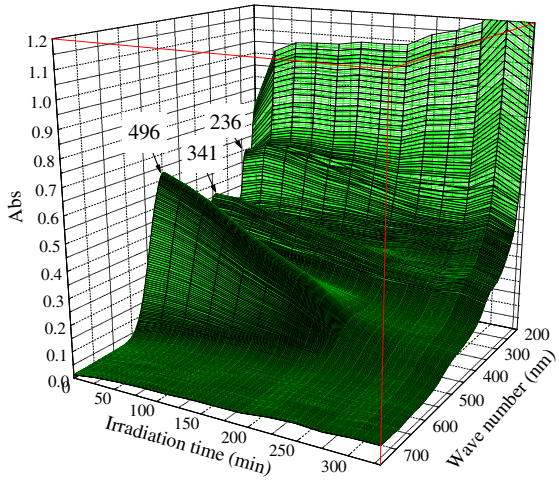

Fig. 8. UV–vis absorption spectra of CR solution during adsorption-photocatalysis (Photocatalyst dosage: 0.5 g L^{-1}; CR concentration: 20 mg L^{-1}).

the first step of the oxidative process [35]. It is interesting to note from Fig. 7 that the absorption maximum of the degraded solution exhibited slight hypsochromic shifts (496–487 nm), which is presumed to result from the formation of a series of N-de-ethylated intermediates in a stepwise manner [36] Similar phenomena were also observed during the photodegradation of CR [5,35] and RhB [37]. In addition to this rapid bleaching effect, the decay of the absorbance at 341 nm was considered as evidence of aromatic fragment degradation in the dye molecule and its intermediates. The excellent activity of the m-alginate/Fe_2O_3/CdS composite may be due to a fast charge separation as a result of the difference in the positions of conduction bands between CdS and Fe_2O_3 [11]. However, the absorbance peaks at 236 nm increased with the increase of irradiation time. This phenomenon may be explained by the formation of intermediate products during the photocatalytic degradation, which have much bigger absorbency than that of original CR molecule [34].

3.4. Effect of initial CR concentration

In this section, a series of CR solutions were prepared, and initial CR concentrations were about 5, 20, 30, and 40 mg L^{-1}, respectively. The photocatalytic degradation of dyes can be described by the Langmuir–Hinshelwood kinetic model. For very low concentrations, the Langmuir–Hinshelwood equation simplifies to a pseudo-first-order kinetic law. The pseudo-first-order rate constants (k_{app}) were calculated from pseudo-first-order plots based on the following Eq. (6):

$$\ln\frac{C_0}{C_t} = k_{app}t \tag{6}$$

where k_{app} is the apparent pseudo-first-order rate constant (min^{-1}), t the irradiation time (min), C_0 is the initial CR concentration (mg L^{-1}), and C_t is the instantaneous dye concentration at t (mg L^{-1}). A plot of ln (C_0/C_i) vs. t will yield a slope of k_{app}.

The relationship between the residual CR concentration (C_t) and the irradiation time (t) photocatalyzed by m-alginate/Fe_2O_3/CdS composite is shown in

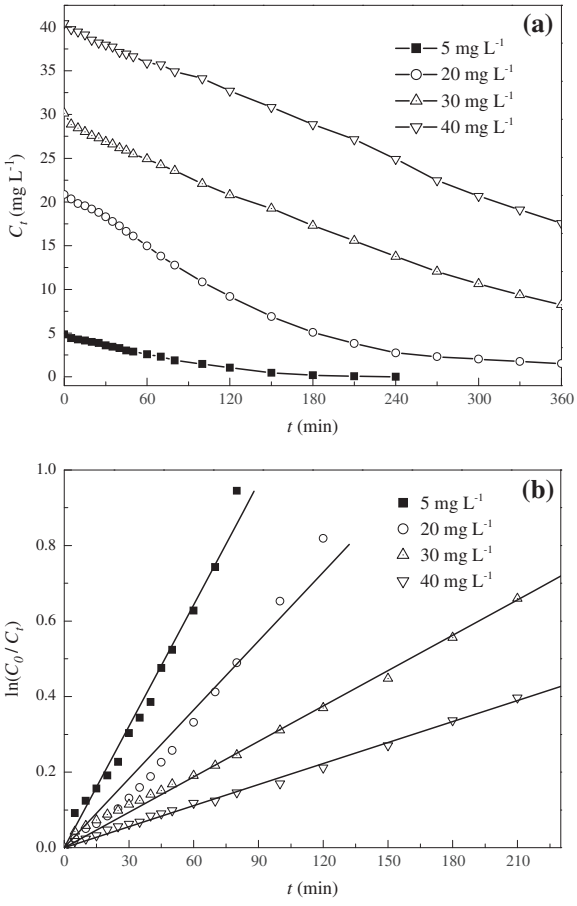

Fig. 9. Effect of initial CR concentration on photocatalytic decolorization by m-alginate/Fe_2O_3/CdS composite (Catalyst dosage: 0.5 g L^{-1}).

Fig. 9(a). After 240 min irradiation, the remanent concentration of CR was 0.00, 2.75, 13.74, and 24.91 mg L^{-1} when initial CR concentration was 5, 20, 30, and 40 mg L^{-1}, respectively. Fig. 9(b) shows the linear plots of $\ln(C_0/C_t)$ vs. irradiation time (t) for various initial CR concentrations. Based on these curves, the degradation reaction rate constants and initial reaction k_{app} were calculated and are summarized in Table 3. The Fig. 9(b) and Table 3 showed that these reactions accorded with a pseudo-first-order kinetic model with high correlation coefficient ($R^2 > 0.991$). The degradation rates obtained were 0.01072, 0.00608, 0.00313, 0.00186 min^{-1}, respectively, for the different initial CR concentrations which were 5, 20, 30, and 40 mg L^{-1}. The kinetic constant for 5 mg L^{-1} of initial concentration was 5.76 times higher than that for 40 mg L^{-1} of initial concentration. The half-life time ($t_{1/2}$) of Langmuir–Hinshelwood analysis provides an additional quantitative comparison for the effect of initial concentration on decoloriztion. The $t_{1/2}$ for 5 mg L^{-1} was about 64.6 min, while $t_{1/2}$ for 40 mg L^{-1} was 372.6 min. Higher the initial CR concentration, longer the time of complete decolorization. An explanation to this phenomenon is that the generation of ·OH radicals on the surface of photocatalyst is reduced at high dye concentrations, since more and more organic substances are adsorbed on the surface of m-alginate/Fe_2O_3/CdS composite and the active sites are covered by dye molecules [38].

Table 3
Parameters for the effect of different initial CR concentrations on the decolorization rate of CR by m-alginate/Fe_2O_3/CdS composite

C_0 (mg L^{-1})	k_{app} (min^{-1})	R^2	$t_{1/2}$[a] (min)
5	0.01072	0.992	64.6
20	0.00608	0.991	114.0
30	0.00313	0.997	221.4
40	0.00186	0.996	372.6

[a]Half-life time.

3.5. Effect of photocatalyst dosage

Photocatalyst amount is another critical parameter to the degradation efficiency. In order to determine the effect of photocatalyst dosage on the degradation of CR, a series of experiments were conducted with varying catalyst dosages from 0.1 to 0.7 g L^{-1}. The results are illustrated in Fig. 10. It is found that the decolorization rate of CR solution increased significantly from 74.83 to 91.54% with an increase of catalyst concentration in the range from 0.1 g L^{-1} to 0.5 g L^{-1} and then decreased to 89.9% with further increase of the catalyst concentration from 0.5 g L^{-1} to

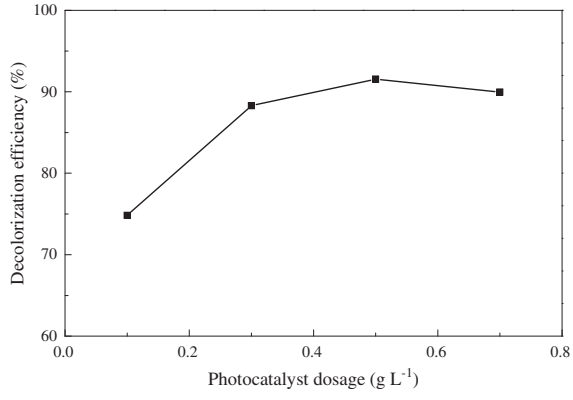

Fig. 10. Effect of photocatalyst dosage on photocatalytic decolorization by m-alginate/Fe_2O_3/CdS composite (CR concentration: 20 mg L^{-1}; irradiation time: 330 min; pH: 5.6).

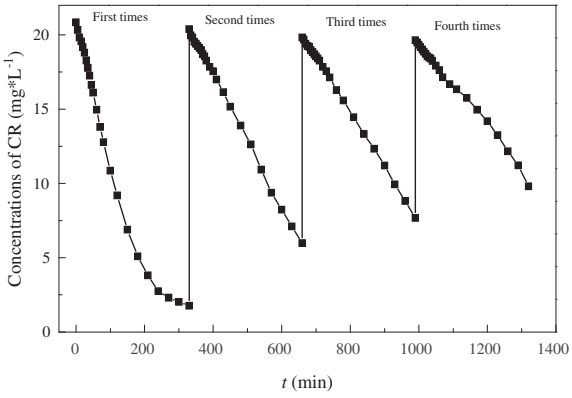

Fig. 11. Effect of recycle time on the decolorization rate of CR solution. (photocatalyst dosage: $0.5\,g\,L^{-1}$; CR concentration: $20\,mg\,L^{-1}$; pH: 5.6).

$0.7\,g\,L^{-1}$. This can be explained in terms of availability of active sites on the photocatalyst surface and the penetration of light into the suspension. At a higher level of photocatalyst concentration, although the reactive sites of photocatalyst increased, the solution became opaque and cloudy, thus reducing the light penetration and leading to the reduction of the availability of active site [39]. In addition, the increase of photocatalyst concentration may result in the agglomeration of the catalyst particles, hence the part of photocatalyst surface became unavailable for photon absorption and dye adsorption, the decolorization rate subsequently decreased. Therefore, there exists an optimum photocatalyst dosage for a given substrate concentration. These phenomena were also observed in other experiments for the photodegradation of aqueous organic dye by polymer-CdS composite photocatalysts [40].

3.6. Reusability of m-alginate/Fe_2O_3/CdS composite

The repeatability of the photocatalytic activity for the photocatalyst is a very important parameter to assess the photocatalyst practicability. To investigate the durability of m-alginate/Fe_2O_3/CdS composite in the reaction, the bleaching experiment was repeated five times. The recovery of photocatalyst was achieved. The concentration of CR was kept constant ($20\,mg\,L^{-1}$) with pH 5.6 and 330 min irradiation time, and the photocatalyst was recovered from treated solution by a magnetic separation technology and subsequent washing with double distilled water three times at every cycle. As displayed in Fig. 11, although the conversion efficiency of CR decreased after each run, the photocatalyst still exhibited activity after four successive cycles under the visible light irradiation. It can been seen that the decolorization rate decreases from 91.2% to 50.9% after four cycles, maintained 55.8% of initial decolorization rate. The decrease of decolorization rate was explained by the loss of m-alginate/Fe_2O_3/CdS composite and the fouling of the photocatalyst by the by-products of degradation. Further research is required to improve the photocatalyst stability.

4. Conclusions

Magnetic alginate/γ-Fe_2O_3/CdS composite photocatalyst (m-alginate/Fe_2O_3/CdS composite) has been successfully fabricated via a simple hydrothermal method. The incorporation of maghemite γ-Fe_2O_3 into the composite semiconductor makes it possible for the m-alginate/Fe_2O_3/CdS composite to be recycled by an external magnetic force. In addition, the m-alginate/Fe_2O_3/CdS composite exhibited efficient photocatalytic activity in the degradation of low concentration aqueous organic dye under visible light irradiation at room temperature. The kinetics of the CR degradation by m-alginate/Fe_2O_3/CdS composite fit well a pseudo-first-order kinetic model. The dye photodecolorization rate increased with the m-alginate/Fe_2O_3/CdS composite concentration up to $0.5\,g\,L^{-1}$, and then decreased with further increasing m-alginate/Fe_2O_3/CdS composite concentration. The decolorization rate maintained 55.8% of initial decolorization rate for fourth cycle.

Acknowledgments

This work is financially supported by the National Natural Science Foundation of China (Grant No. 21007044 and 51208331) and the Domestic Visitor Foundation for Outstanding Young Teachers in the Higher Education Institutions from the Education Ministry of China).

References

[1] G. Annadurai, R.S. Juang, D.J. Lee, Factorial design analysis for adsorption of dye on activated carbon beads incorporated with calcium alginate, Adv. Environ. Res. 6 (2002) 191–198.
[2] H.Y. Zhu, R. Jiang, L. Xiao, G.M. Zeng, Preparation, characterization, adsorption kinetics and thermdynamics of novel magnetic chitosan enwrapping nanosized γ-Fe_2O_3 and multi-walled carbon nanotubes with enhanced adsorption properties for methyl orange, Bioresour. Technol. 101 (2010) 5063–5069.
[3] P. Kumar, R. Agnihotri, K.L. Wasewar, H. Uslu, C.K. Yoo, Status of adsorptive removal of dye from textile industry effluent, Desalin. Water Treat. 50 (2012) 226–244.
[4] H.Y. Zhu, L. Xiao, R. Jiang, G.M. Zeng, L. Liu, Efficient decolorization of azo dye solution by visible light-induced photocatalytic process using SnO_2/ZnO heterojunction immobilized in chitosan matrix, Chem. Eng. J. 172 (2011) 746–753.

[5] H. Zhu, R. Jiang, L. Xiao, Y. Chang, Y. Guan, X. Li, G. Zeng, Photocatalytic decolorization and degradation of congo red on innovative crosslinked chitosan/nano-CdS composite catalyst under visible light irradiation, J. Hazard. Mater. 169 (2009) 933–940.
[6] S.M. Lam, J.C. Sin, A.Z. Abdullah, A.R. Mohamed, Degradation of wastewaters containing organic dyes photocatalysed by zinc oxide: A review, Desalin. Water Treat. 169 (2009) 933–940.
[7] V. Golab, A. Vinder, M. Simonic, Efficiency of the coagulation/flocculation method for the treatment of dye bath effluent, Dyes Pigm. 67 (2005) 93–97.
[8] J. Colina-Máquez, F. Machuca-Martínez, G.L. Puma, Radiation absorption and optimization of solar photocatalytic eeactors for environmental applications, Environ. Sci. Technol. 44 (2010) 5112–5120.
[9] D. Ke, S. Liu, K. Dai, J. Zhou, L. Zhang, T. Peng, CdS/regenerated cellulose nanocomposite films for highly efficient photocatalytic H_2 production under visible light irradiation, J. Phys. Chem. C 113 (2009) 16021–16026.
[10] R. Jiang, H. Zhu, J. Yao, Y. Fu, Y. Guan, Chitosan hydrogel films as a template for mild biosynthesis of CdS quantum dots with highly efficient photocatalytic activity, Appl. Surf. Sci. 258 (2012) 3513–3518.
[11] L. Wang, H. Wei, Y. Fan, X. Gu, J. Zhan, One-dimensional CdS/α-Fe_2O_3 and CdS/Fe_3O_4 heterostructures: Epitaxial and nonepitaxial growth and photocatalytic activity, J. Phys. Chem. C 113 (2009) 14119–14125.
[12] J. Zeng, S. Liu, J. Cai, L. Zhang, TiO_2 immobilized in cellulose matrix for photocatalytic degradation of phenol under weak UV light irradiation, J. Phys. Chem. C 114 (2010) 7806–7811.
[13] H. Zhu, R. Jiang, Y. Guan, Y. Fu, L. Xiao Ling, G. Zeng, Effect of key operational factors on decolourization of methyl orange during H_2O_2 assisted nanosized CdS/TiO_2/polymer composite thin films under simulated solar light irradiation, Sep. Purif. Technol. 74 (2010) 187–194.
[14] W. Albert, H. Mau, C. Huang, N. Kakuta, A.J. Bard, A. Campion, M.A. Fox, J.M. White, S.E. Webber, Hydrogen photoproduction by Nafion/cadmium sulfide/platinum films in water/sulfide ion solutions, J. Am. Chem. Soc. 106 (1984) 6537–6542.
[15] U. Wendy, J. Janke, J. Dittmer, A.P. Alivisatos, Hybrid nanorod-polymer solar cells, Sci. 295 (2002) 2425–2427.
[16] A.-F. Ngomsik, A. Beea, J.-M. Siauguea, V. Cabuila, G. Coteb, Nickel adsorption by magnetic alginate microcapsules containing an extractant, Water Res. 40 (2006) 1848–1856.
[17] J. Bajpai, R. Shrivastava, A.K. Bajpai, Dynamic and equilibrium studies on adsorption of Cr(VI) ions onto binary biopolymeric beads of cross linked alginate and gelatin, Colloids Surf. A 236 (2004) 81–90.
[18] T.Y. Kim, H.J. Jin, S.S. Park, S.J. Kim, S.Y. Cho, Adsorption equilibrium of copper ion and phenol by powdered activated carbon, alginate bead and alginate-activated carbon bead, J. Ind. Eng. Chem. 14 (2008) 714–719.
[19] S.K. Papageorgiou, F.K. Katsaros, E.P. Kouvelos, N.K. Kanellopoulos, Prediction of binary adsorption isotherms of Cu^{2+}, Cd^{2+} and Pb^{2+} on calcium alginate beads from single adsorption data, J. Hazard. Mater. 162 (2009) 1347–1354.
[20] T. Gotoh, K. Matsushima, K.-I. Kikuchi, Adsorption of Cu and Mn on covalently cross-linked alginate gel beads, Chemosphere 55 (2004) 57–64.
[21] R. Wu, J. Qu, H. He, Y. Yu, Removal of azo-dye Acid Red B (ARB) by adsorption and catalytic combustion using magnetic $CuFe_2O_4$ powder, Appl. Catal. B 48 (2004) 49–56.
[22] J.W. Liu, Y. Zhang, D. Chen, T. Yang, Z.P. Chen, S.Y. Pan, N. Gu, Facile synthesis of high-magnetization γ-Fe_2O_3/alginate/silica microspheres for isolation of plasma DNA, Colloids Surf. A 341 (2009) 33–39.
[23] T. Zhang, H. Luo, H. Zeng, R. Zhang, Y. Shen, Synthesis and gas-sensing characteristics of high thermostability γ-Fe_2O_3 powder, Sens. Actuators, B 32 (1996) 181–184.
[24] H. Jia, H. Xu, Y. Hu, Y. Tang, L. Zhang, TiO_2@CdS core–shell nanorods films: Fabrication and dramatically enhanced photoelectrochemical properties, Electrochem. Commun. 9 (2007) 354–360.
[25] L. Fan, Y. Du, R. Huang, Q. Wang, X. Wang, L. Zhang, Preparation and characterization of alginate/gelatin blend fibers, J. Appl. Polym. Sci. 96 (2005) 1625–1629.
[26] G. Yang, L.N. Zhang, T. Peng, W. Zhong, Effects of Ca^{2+} bridge cross-linking on structure and pervaporation of cellulose–alginate blend membrane, J. Membr. Sci. 175 (2000) 53–60.
[27] S.W. Cao, Y.J. Zhu, Y.P. Zeng, Formation of -Fe2O3 hierarchical nanostructures at 500˚C in high magnetic field, J. Magn. Magn. Mater. 321 (2009) 3057–3060.
[28] Z.H. Jing, Synthesis, characterization and gas sensing properties of undoped and Zn-doped Fe2O3-based gas sensors, Mater. Sci. Eng. A 441 (2006) 176–180.
[29] C. Xiao, L. Weng, L. Zhang, Improvement of physical properties of crosslinked alginate and carboxymethyl konjac glucomannan blend films, J. Appl. Polym. Sci. 84 (2002) 2554–2560.
[30] B.D. Cullity, Introduction to Magnetic Materials, Addison-Wesley, Reading, MA,. 201 1972.
[31] A. Corma, F.J. Ortega, Influence of adsorption parameters on catalytic cracking and catalyst decay, J. Catal. 233 (2005) 257–265.
[32] S. Lagergren, Zur theorie der sogenannten adsorption geloster stoffe [About the theory of so-called adsorption of soluble substances], Kungl. Svenska Vetenskapsakademiens. Handlingar, Band 24 (1898) 1–39.
[33] Y.S. Ho, G. McKay, Sorption of dye from aqueous solution by pit, Chem. Eng. J. 70 (1998) 115–124.
[34] J. Wang, R.H. Li, Z.H. Zhang, W. Sun, R. Xu, Y.P. Xie, Z.Q. Xing, X.D. Zhang, Efficient photocatalytic degradation of organic dyes over titanium dioxide coating upconversion luminescence agent under visible and sunlight irradiation, Appl. Catal. A-Gen. 334 (2008) 227–233.
[35] N.J. Bejarano-Pérez, M.F. Suárez-Herrera, Sonophotocatalytic degradation of congo red and methyl orange in the presence of TiO_2 as a catalyst, Ultrason. Sonochem. 14 (2007) 589–595.
[36] N. Modirshahla, M.A. Behnajady, Photooxidative degradation of Malachite Green (MG) by UV/H_2O_2: Influence of operational parameters and kinetic modeling, Dyes Pigm. 70 (2006) 54–59.
[37] W. Zhao, C.C. Chen, X.Z. Li, J.C. Zhao, H. Hidaka, N. Serpone, Photodegradation of sulorhodamine-B dye in platinum as a functional co-catalyst, J. Phys. Chem. B 106 (2002) 5022–5028.
[38] A. Nageswara Raoa, B. Sivasankarb, V. Sadasivam, Kinetic study on the photocatalytic degradation of salicylic acid using ZnO catalyst, J. Hazard. Mater. 166 (2009) 1357–1361.
[39] A. Akyol, H.C. Yatmaz, M. Bayramoğglu, Photocatalytic decolourization of Remazol Red (RR) in aqueous ZnO suspensions, Appl. Catal. B: Environ. 54 (2004) 19–24.
[40] R. Jiang, H. Zhu, X. Li, L. Xiao, Visible light photocatalytic decolourization of C. I. Acid Red 66 by chitosan capped CdS composite nanoparticles, Chem. Eng. J. 152 (2009) 537–542.